

# Study on Pullout Behavior of Uniaxial HDPE Geogrids Under Monotonic and Cyclic Loads

Arash Nayeri<sup>1</sup>, Kazem Fakharian<sup>2,\*</sup>

Received: December 2008

Accepted: November 2009

**Abstract:** This paper presents the results of pullout tests on uniaxial geogrid embedded in silica sand under monotonic and cyclic pullout forces. The new testing device as a recently developed automated pullout test device for soil-geogrid strength and deformation behavior investigation is capable of applying load/displacement controlled monotonic/cyclic forces at different rates/frequencies and wave shapes, through a computer closed-loop system. Two grades of extruded HDPE uniaxial geogrids and uniform silica sand are used throughout the experiments. The effects of vertical surcharge, sand relative density, extensibility of reinforcement and cyclic pullout loads are investigated on the pullout resistance, nodal displacement distributions, post-cyclic pullout resistance and cyclic accumulated displacement of the geogrid. Tell-tale type transducers are implemented along the geogrid at several points to measure the relative displacements along the geogrid embedded length. In monotonic tests, decrease in relative displacement between soil and geogrid by increase of vertical stress and sand relative density are the main conclusions; structural stiffness of geogrid has a direct effect on pullout resistance in different surcharges. In cyclic tests it is observed that the variation of post-cyclic strength ranges from minus 10% to plus 20% of monotonic strength values and cyclic accumulated displacements are increased as normal pressure increase, but no practical specific comment can be made at this stage on the post-cyclic strength of geogrids embedded in silica sand. It is also observed that in loose sand condition, the cyclic accumulated displacements are considerably smaller as compared to dense sand condition.

**Keywords:** Pullout box; Silica Sand; Geogrid; Pullout resistance; Cyclic load; Post-cyclic resistance.

## 1. Introduction

In the limit state design procedure, external and internal stability of the reinforced systems such as earth walls has to be proven. External stability includes control of overturning, sliding and bearing capacity failures and the internal stability includes tensile failure, connection failure and pullout failure of reinforcement embedded in soil. The internal instability may occur as a result of increase in total force in reinforcement in excess of the pullout resistance in the anchorage zone of the embedded reinforcing element in soil.

Geogrids, as one of the members of geosynthetics family, are widely used as reinforcement in earth structures and in

particular, HDPE geogrids have gained popularity because of their adequate pullout resistance. The pullout resistance that is established with respect to an interaction factor describing the interface bond mobilized between the geogrid and the soil is constituted of two components: frictional resistance between soil and geogrid surface [1] and the bearing resistance of soil in front of the ribs. [2,3]

Pullout box is a common practice to investigate the pullout behavior of reinforcement embedded in soil, as an element testing apparatus. The testing apparatus is basically comprised of a box with rigid walls, arrangements for application of normal pressure and horizontal pullout load, frontal clamp and external (and sometimes internal) measurement devices. Table 1 presents the main characteristics of most of the pullout boxes reported in the literature.

Many studies are reported in literature to study the effect of various parameters on monotonic pullout behavior of geogrids, for example effect of rigidity and flexibility of the face [4], [5], [6], effect of different mechanisms for application of

\* Corresponding author. Email: kfakhari@aut.ac.ir

1 Ph.D. Student, Department of Civil and Environmental Engineering, Amirkabir University of Technology, Tehran, Iran

2 Assistant Professor, Department of Civil and Environmental Engineering, Amirkabir University of Technology, Tehran, Iran

**Table 1.** Summary of pullout test apparatus and materials characteristics

Reference	Box Dimensions (mm)	Soil Characteristics		Soil preparation	Surcharge (kPa)
		Soil Type	C (kPa) – $\phi$ (°) Grain size (mm)		
Bonczkewicz & Christopher (1987)	1325×675×150	Sand-silt	$\phi$ =35-43 PI=6-21	vibrator	35-70-100
Ochiai & Otani (1992)	600×400×400	Sand	$\phi$ =36	pluviation	25-50-75
Collin & Berg (1993)	2100×900×500	Sand-SP	$\phi$ =28	compaction	49-100
Yasuda & Marui (1993)	500×300×100	Volcanic ash	$\phi$ =28-36 $D_1$ =30%	compaction	20-100
Farrag & Griffin (1993)	1500×900×760	Clay	PI=24	vibrator	48.2
Razaqpur & Bauer (1993)	1040×230×380	Crushed stone	$\phi$ =36-40 $D_{50}$ =8mm	compaction	14-20
Wilson-Fahmy & Koerner (1993)	1900×9100×110	Sand	$\phi$ =49 $D_{50}$ =0.7mm	compaction	10-25 51-100
Alfaro & Bergado (1995)	3230×700×700	Gravel-GW	$\phi$ =41-45	compaction	20-30-50
Lechshinsky & Kaliakin (1995)	600×200×300	Ottawa sand	$\phi$ =40 $D_{50}$ =0.25	pluviation	17.2-34.2 51-70-100
Raju & Fannin (1998)	3230×700×700	Sand	$\phi$ =36 $D_{50}$ =0.9	compaction	4-20
Lopes & Lopes (1999)	1530×1000×800	Sand-gravel	$\phi$ =40 $D_{50}$ =1.2mm	compaction	50-100-200
Bolt & Duzynska (2000)	1600×600×360	Quartz	$\phi$ =28-36	compaction	25-50-100
Sugimoto & Alagiawanna (2003)	680×300×625	Sand	$\phi$ =30 $D_{50}$ =0.34	pluviation	5-49-93
Nernheim & Meyer (2003)	1500×600×700	Sand-SP	$\phi$ =30-43	pluviation	30-45-60
Moraci & Recalcati (2004)	1700×600×680	Sand-SP	$\phi$ =42-48 $D_{50}$ =1.20	compaction	10-25 50-100
Fakharian & Nayeri (2007)	1200×600×600	Silica sand	$\phi$ =34-40 $D_{50}$ =1.20	pluviation	15-25 50-100

vertical pressure [7], effect of soil thickness and sample geometry [8], effect of reinforcement clamp and casing [9], [10], and effect of longitudinal and rib elements on pullout strength [6], [11]. The displacement-controlled monotonic loading has been applied to the geogrid specimen in most of the above studies.

Geogrids used for earth reinforcement are subjected not only to static loads but also to cyclic loads. The cyclic loads may be resulted from traffic loading on highway embankments and reinforced bridge abutments, railways, machinery foundations, impact load of ships in costal structures and wave loads on protected

slopes. Such cyclic loads or surcharges induce cyclic tensile forces in reinforcing elements in addition to the static forces.

In the absence of sufficient experimental results, some researchers proposed a reduction factor of 0.8 on pullout resistance as a result of dynamic loads [12]. The effect of normal cyclic surcharges on pullout behavior of geogrids in sand was studied by Yasuda et al. [13] and concluded that the pullout resistance not only is dependent on the soil type and normal pressure, but also under cyclic normal pressure is greater than pullout strength under static normal pressure. They observed that pullout resistance under normal cyclic surcharge, decreases with increase in the cyclic amplitude. Raju and Fannin [14], studied two types of geogrids under static and cyclic pullout loads. They concluded that as opposed to the common design practice, with increase in loading amplitude, the relative displacements at the zone near the clamp increases, but the distribution is not uniform along the specimen. They also found that depending on the surcharge magnitude and geogrid type, the static and cyclic resistances are not necessarily equivalent, but exhibit no consistent trend. The general trend is the occurrence of pullout failure under cyclic loads due to accumulation of displacements in the reinforcement. The trend of accumulation of displacement with increase in number of cycles in pullout tests of metal belt and geogrids have been studied by Nernheim and Meyer [15]. For embedded geogrids, the induced displacement is greater than the metal belt, but no failure has been observed, even at large number of cycles.

Evaluation of the available results in literature shows that the effect of cyclic loading on pullout resistance is not sufficiently studied yet. For example, the influence of many parameters such as soil gradation and relative density, geogrid type and loading path, that is understood are having significant effects in monotonic loading condition, are not studied under cyclic pullout tests yet.

The main objective of this study is to investigate the effects of various parameters on the pullout resistance and accumulation of displacements of sand-geogrid under cyclic loading conditions.

Effects of normal pressure, geogrid stiffness, soil relative density, and type of loading path, are investigated during a general loading process including monotonic, cyclic and post-cyclic loads on geogrids embedded in silica sand.

## **2. Experiments**

### **2.1. Apparatus**

The pullout apparatus has been recently developed in Amirkabir University of Technology, Department of Civil and Environmental Engineering. It constitutes of the pullout box, hydraulic actuator for applying the pullout force, surcharge pressure setup and instrumentation arrangements for load and displacement measurements. A closed-loop computer-controlled system enables application of all loading patterns including monotonic and cyclic loads. Some details are presented in the following sections.

#### **2.1.1. Pullout box**

The pullout box is designed to have inside dimensions of 1200 mm length, 600 mm width and 600 mm height that are selected based on standard requirements [16]. The developed box is fixed at the bottom to a grid-type pad, constructed using I-profiles, to distribute the weight of equipments more uniformly to the laboratory floor. ST-37 steel plates with 15 mm thickness are used to assemble the main box. Vertical stiffeners on the rear and side plates of the box are used to prevent buckling or excessive displacements at mid-height of faces during testing. The top cover plate is supported by two hinges and two fasteners to ensure the safety and convenience during opening and closing. All the connections are either welded or bolted, depending on the performance requirements. The schematics of plan and elevation views of apparatus are illustrated in Fig. 1. The pullout setup is arranged within boundaries of the box. This may not be well representative of the full-scale real life problems in that side frictions can significantly affect the pullout behavior and to minimize this effect, smooth acrylic plates are placed on the internal face of two rear walls.

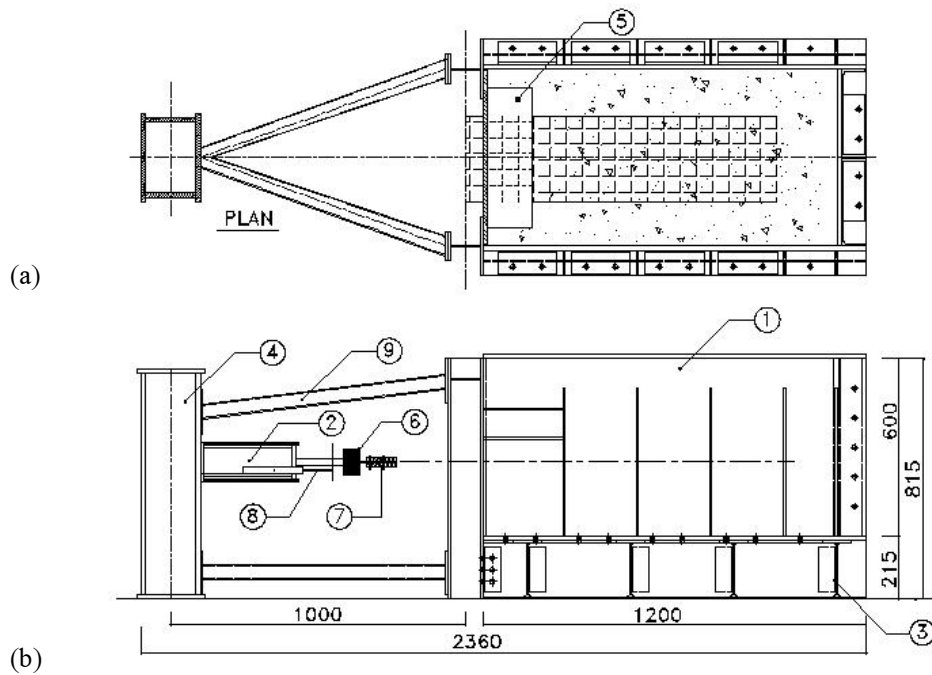


Fig. 1. (a,b) Schematic details of the pullout test apparatus.

(1) main box; (2) hydraulic actuator; (3) grid-type pad; (4) hydraulic jack support; (5) reinforcement casing; (6) load cell; (7) clamp; (8) LVDT; (9) reaction elements

### 2.1.2. Reinforcement clamp and casing

Two parallel plates,  $500 \times 200 \times 10$  mm each, are mounted horizontally above and below the inside front box groove, as shown in Fig. 2(a). The plates are covering the reinforcement specimen like a casing, enabling the pullout force to be transmitted to the embedded geogrid in soil through a distance equivalent to the casing width of 200 mm, reducing the pressure on the box front, and reducing the friction effect of the front plate on the specimen behavior.

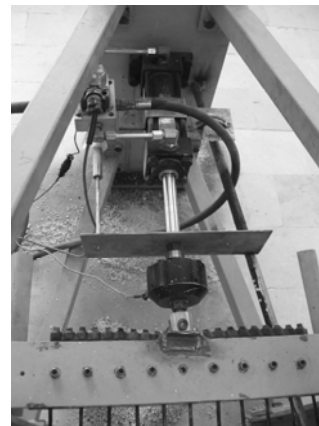
The reinforcing specimen is grabbed by two  $100 \times 10$  mm belts, tightened to each other by 9 bolts, as shown in Fig. 2(b). This clamp is connected to the pulling force arrangement at the other end and is expected to uniformly distribute the pullout force across the width of specimen.

### 2.1.3. Hydraulic actuator and airbag

A 50 kN hydraulic jack with 100 mm stroke is utilized to apply the horizontal load. A loadcell with proper capacity is mounted between the hydraulic actuator and the reinforcement clamp as shown in Fig. 2(b). A closed-loop computer-



(a)



(b)

Fig. 2. Pullout apparatus details:

(a) reinforcement casing, (b) clamp and actuator system

controlled servo system is used to operate the hydraulic jack, through getting feedback from either loadcell or displacement transducer, to apply the user-defined load or displacement paths. Monotonic loading at various rates and cyclic loading with frequencies of very small to as high as 20 Hz and different wave shapes, either displacement- or load-controlled can also be generated. The hydraulic actuator and the load measurement components are hold up by a vertical box-section pier supported by four compressive elements connected to the front of the box to control and transfer the compression forces to the main body as illustrated in Fig. 1(b).

Five LVDTs are used to measure the displacements at four different points along the embedded length of specimen and one point on clamp to measure the so-called, frontal displacement. Non-extensible wires enclosed by stainless steel casing, are connecting the rib elements along the geogrid to the LVDTs mounted behind the box. The vertical pressure on the top of the soil is generated using an airbag designed to sustain pressures over 150 kPa. A regulated air line is attached to the airbag to maintain the user-defined normal pressure constant during the test, even if air is in/out due to dilative/contractive effects.

Two sets of reticulated steel tray are made for air-pluviation of silica sand for coarse- and fine-grain soil types. Falling height during pluviation is adjusted to 600 mm for preparing dense sand and it is reduced to 50 mm for achieving loose

sand samples.

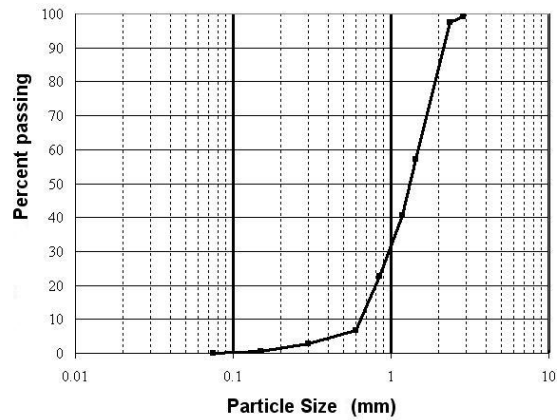
## 2.2. Materials

### 2.2.1. Reinforcement

Two types of extruded HDPE geogrids, namely G1 (Tenax TT 060 SAMP) and G2 (Tenax TT 120 SAMP) are used and the general geometry and strength properties of two types of geogrids are presented in Table 2.

### 2.2.2. Sand

Silica sand with angular particles having  $D_{50}$  of 1.2 mm and grain-size distribution of Fig. 3 is used during the experiments. Direct shear tests



Silt	Sand			Gravel
	Fine	Medium	Coarse	Fine

Fig. 3. Silica sand particle size distribution,

Table 2. Geometry and strength properties of geogrids

Characteristic	G1	G2
Aperture size MD, longitudinal (mm)	220	220
Aperture size TD, transverse (mm)	13/20	13/20
Strength at 2% strain (kN/m)	17	36
Peak tensile strength (kN/m)	60	120
Yield point elongation (kN/m)	13	13

MD: machine direction (longitudinal to the roll)

TD: transverse direction (across roll width)

**Table 3.** General properties of silica sand

Characteristic	Value
Dry unit weight, $\gamma_d$ (kN/m <sup>3</sup> )	16
Max. void ratio, $e_{max}$	0.95
Min. void ratio, $e_{min}$	0.67
D <sub>50</sub> (mm)	1.20
Uniformity coefficient, $C_u$	1.30
Internal friction angle: Loose	32
Dense	36

have provided an average friction angle of 36° on dense samples and about 32° in loose condition. Table 3 presents the physical properties as well as the strength parameters for the silica sand.

### 2.3. Test procedure

The pullout test procedure is described below:

(1) Considering of 100 mm for thickness of the airbag, 500 mm is left for placing sand and embedding reinforcement. The sand is pluviated in two 125 mm layers to reach the elevation of the casing plate and then final grade is leveled off at mid height of the box centered to the front groove.

(2) The geogrid sample is placed on the soil surface, the front of which is passed through the front box groove and fixed to the clamps (Fig. 4). Relative displacement of four transverse ribs of geogrids are measured by four non-extensible



**Fig. 4.** Sample preparation and installation of nodal displacement measurement system

wires connected to the ribs and passed through steel casing to connect to an LVDT set-up system.

(3) The two other 125 mm sand layers are placed and the top surface is perfectly leveled at 500 mm elevation and the airbag is placed on top of the soil surface.

(4) The top lid is closed and secured by two or three fasteners, depending on intensity of normal pressure. The airbag is then pressurized and regulated at the target pressure. It requires a few minutes to establish the target normal pressure.

(5) The pullout force is normally applied in a displacement-controlled manner by a fully closed-loop control system at constant rates of 1 mm/min. The test is terminated when a pullout failure is occurred, the geogrid is damaged, or a frontal displacement of 100 mm is reached.

In cyclic tests, the loading procedure is divided into several steps including the initial monotonic step up to load  $T_1$  and then cycles would start.  $T_1$  and the amplitude of cycles,  $T_a$ , are specified as a defined percentage of the ultimate monotonic pullout resistance,  $T_u$ , in this study.

### 3. Tests Outline

In this study, the results of monotonic tests are presented first as a benchmark to compare with the cyclic test results. The monotonic loading in pre- and post-cyclic steps were performed at a rate of 1 mm/min under different surcharges, using two geogrid types of G1 and G2 and both loose and dense sand conditions. In cyclic tests, loading level at start of cyclic load and its amplitude,  $T_1$  and  $T_a$ , are shown in the legend of each graph as the test specification. In most of the tests,  $T_1/T_u=0.6$  and  $T_a/T_u=0.4$  are specified. Cyclic loading has continued up to 100 cycles with frequency of 0.1 Hz in all the tests. After the last cycle, the post-cyclic loading in a displacement-controlled manner has started and continued up to the end of test.

## 4. RESULTS

### 4.1. Monotonic test results

Variation of pullout force versus frontal

displacement of geogrids G1 and G2 embedded in dense and loose sand are presented in Fig. 5.

Figures 5(c, f) show the trend of maximum pullout resistance of two type geogrids vs. the

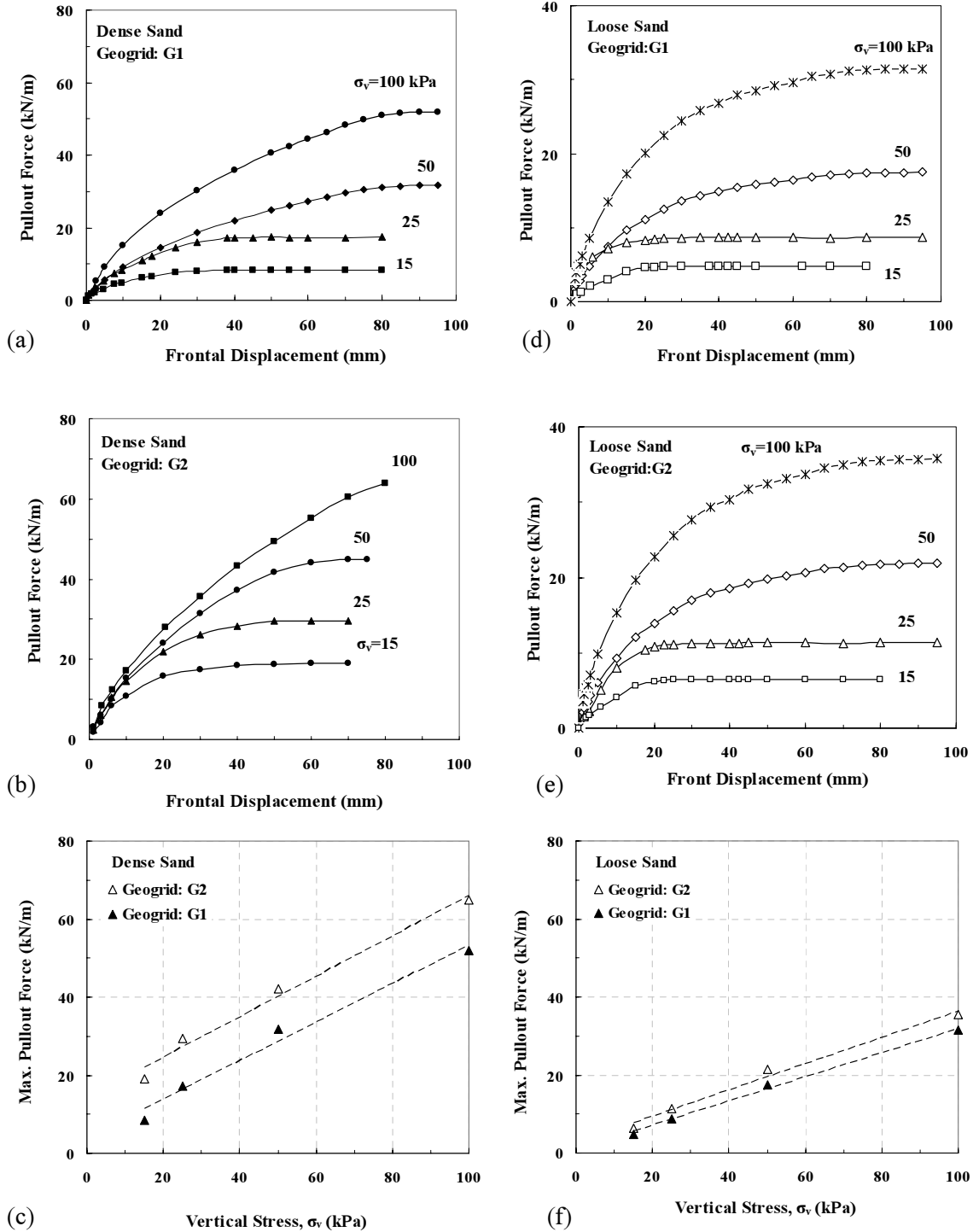


Fig. 5. (a,b,c) Monotonic pullout resistance of geogrids G1 and G2 in dense sand  
(d,e,f) Monotonic pullout resistance of geogrids G1 and G2 in loose sand

vertical surcharge in dense and loose sand conditions. According to Figs. 5(a, b, d, e) the initial stiffness of both types of geogrids G1 and G2 and their maximum pullout resistance increases with increase of vertical stress, as expected. Pullout resistance increases significantly, as the relative density increases from 45% in loose sample to 90% in dense condition. Such observations could be assessed by increasing the soil angle of internal friction and interlocking of soil particles in the aperture zone of geogrid, with increase in soil relative density and intensity of vertical stress. The results confirm the important contribution of soil bearing capacity in front of the transverse ribs in total pullout resistance of uniaxial geogrids such as pullout force decreases about 80% in different normal surcharge, when shifting from dense to loose sand, reducing the relative density to half.

Similar results in monotonic tests have been reported in the literature, but monotonic results of this study highlight the sensitivity of pullout resistance mobilization to load-strain characteristic of geogrids with near-similar geometrical structure. As seen in Fig. 5(c), at each surcharge, the absolute amount of pullout resistance difference between G2 and G1 is about 12kN/m. This corresponds to a relative difference of 80% for lower surcharges (15 kPa), and 17% in high surcharges (100 kPa) for dense sand. In other words, the relative difference in pullout resistance for G1 and G2, decreases as surcharge increases. The physical interpretation of the observed behavior is attributed to the extensibility of the geogrids. Geogrid G2, with half stiffness of G1, shows inextensible behavior under low surcharges and this induces an immediate development of interaction mechanism. But G1 is more extensible than G2 under low surcharges, resulting in lower pullout resistance in same frontal displacements. On the other hand, under high surcharges, mobilization of friction and bearing resistance is progressive, thus the difference in pullout resistance for G1 and G2, originates from the difference in effective bearing area of transverse ribs, and tensile strength of geogrids has little role in providing the pullout resistance.

## 4.2. Cyclic test results

The pullout behavior of geogrids under different loading paths is important in both strength and deformation related aspects. The first aspect includes the maximum pullout force, load-displacement relations, failure pattern, and effect of cyclic loads on interaction behavior. In the second aspect which is deformation related, the maximum displacement at the pullout resistance load, the mobilized strains along the embedded length of geogrid and their distribution pattern, accumulation of displacements during cyclic loads and effect of characteristics of dynamic loading on displacements are studied. Some of distinguished points of these two aspects are investigated in the subsequent sections.

### 4.2.1 Strength related results

Two sets of experiments from the entire laboratory program, including geogrid G2 embedded in loose and dense state of silica sand are selected to investigate cyclic response of reinforcement under different vertical surcharges. Fig. 6 shows load-displacement variations of geogrid G2 under different surcharges in dense and loose state of silica sand. The solid lines show the pre- and post-cyclic portions which were performed using displacement-controlled loading and the dotted lines are the monotonic response of each situation. Overall observation so far is little variation under different surcharges. Post-cyclic monotonic response exhibits some increase in the initial stiffness right after cycles that is probably attributed to the sand densification with cycles.

With increasing vertical pressure, monotonic resistance,  $T_u$ , increase, therefore  $T_1$  and  $T_a$  as a portion of ultimate monotonic resistance will be increased. For higher  $T_1$  values, at the commencement of cyclic loads, large frontal displacement occurs leading to the mobilization of significant portion of friction and bearing resistance; therefore, during post-cyclic loading, the pullout resistance is lower than monotonic loading and larger accumulated displacement during 100 cycles is observed. At low amplitude



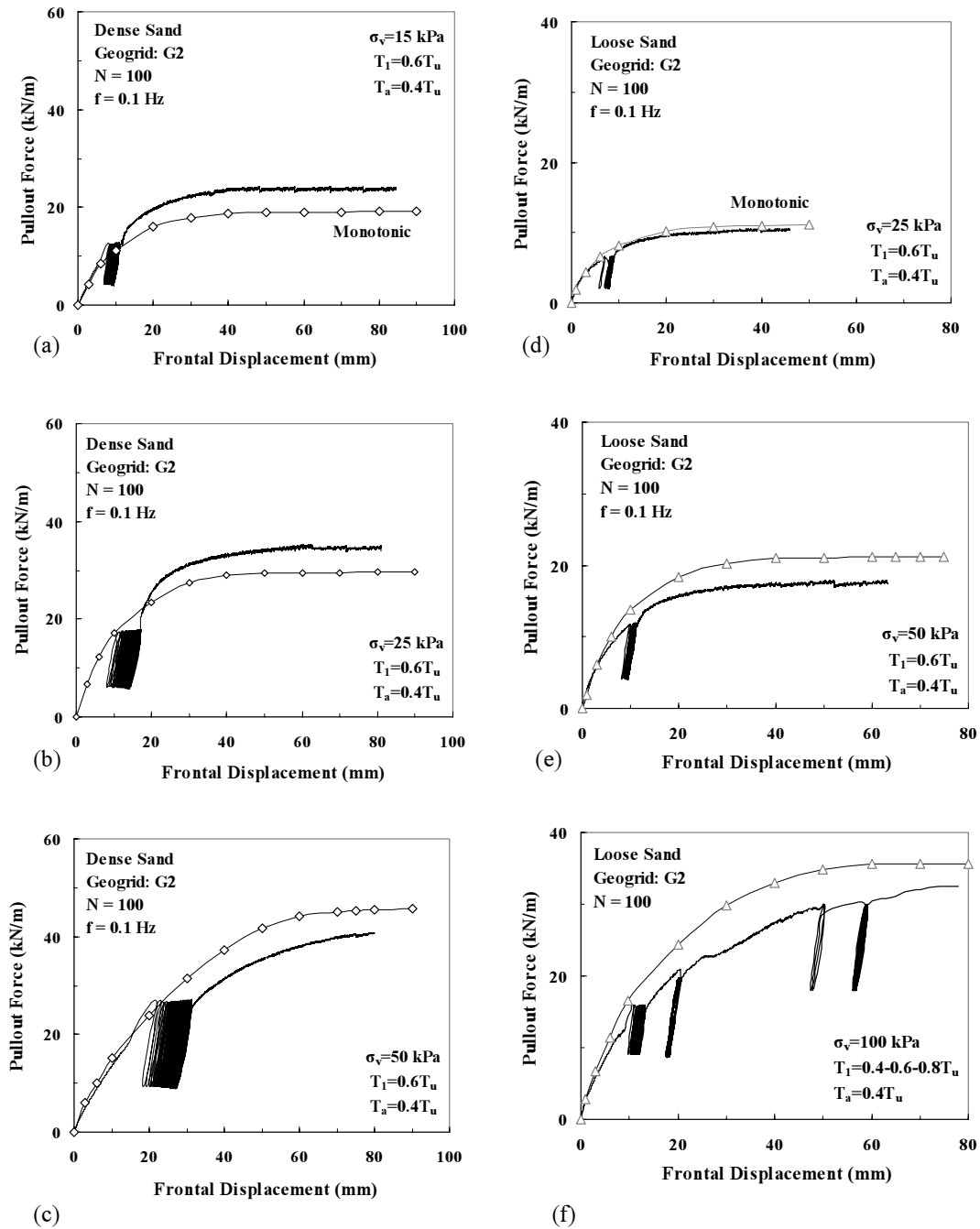


Fig. 6. (a,b,c) Cyclic pullout behavior of geogrid G2 in dense silica sand  
(d,e,f) Cyclic pullout behavior of geogrid G2 in loose silica sand

cyclic pullout loads values, sand particles are not rearranged; hence, a pullout resistance equal to, or about 10% greater than monotonic values are observed. By increasing the loading amplitude under greater surcharges, degradation of the bearing soil structure in front of transverse ribs

increases and this in turn reduces the ability of sand to mobilize the initial monotonic resistance in post-cyclic conditions. Figure 7(a) shows the trend of post-cyclic relationship vs. normal surcharges. For loose sand condition, except in one case, the post-cyclic strength slightly

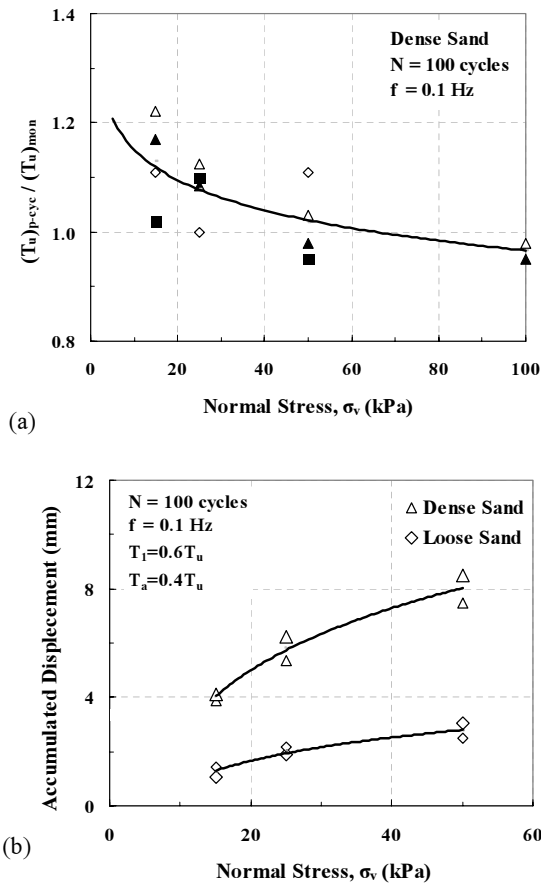


Fig. 7. (a) Effect of surcharge on post-cyclic resistance  
(b) Effect of surcharge on accumulated displacement

decreased compared to monotonic loading, but no particular trend is observed in the results presented.

Another important cyclic loading pattern is loading/unloading cycles such as the one shown in Fig. 8. The experiment includes nine complete unloading/reloading cycles, i.e. unloading to zero load during each cycle. The unloading/reloading slopes may be used as pullout load-displacement stiffness for design purposes. The slopes at different load levels are almost similar and although the ultimate strength has increased about 25 percent compared to monotonic resistance, it should be noted that repetition of cycles can result in displacement instability of reinforcement.

#### 4.2.2 Displacement behavior

The effect of cyclic loading on the total cyclic accumulated displacement for certain number of

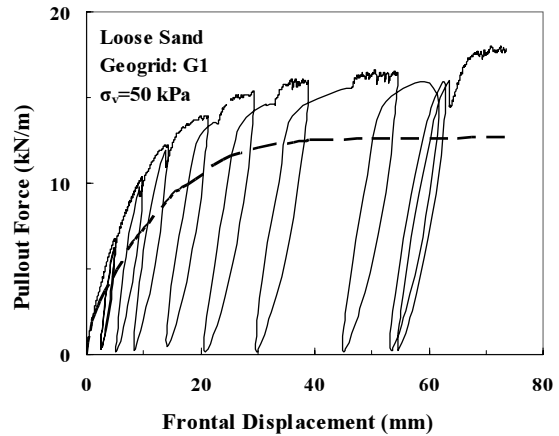


Fig. 8. Loading/unloading pattern effect on pullout behavior of geogrid G1 in loose sand

cycles, and distribution of displacements and strains along the embedded length of geogrid are specific points evaluated in this section. Figure 6 shows that in dense sand, with increase in the vertical stress, but the same loading pattern and number of cycles, the accumulated displacements of geogrid have significantly increased. Fig. 7(b) compare the variation of cyclic accumulated displacements vs. surcharges for dense and loose sand conditions and it is clear that accumulated displacements for loose samples are smaller compared to dense sand condition.

It was expected to observe higher accumulation of displacement with cycles for sand in loose state compared to dense sand under identical loading patterns. The observations are opposite, however. It is noticed that for the same loading pattern and geogrid type, the average accumulation of displacements in dense condition is about up to 100% higher as compared to loose condition, as could be confirmed from Fig. 7(b). It is difficult to explain this behavior, but one important possibility is the fact that in the loose state of sand, the  $T_1$  of  $0.6T_u$  starts at a much lower state of force, because the ultimate resistance of embedded geogrid in dense sand is almost double of the loose sand condition. More test data are required to conclude on this observation.

Figure 9 shows the increase in displacement with log. of number of cycles for reinforcement G2 embedded in dense sand. The initial displacement is highly dependent on  $T_1$  at start of cyclic loading and its amplitude, but the

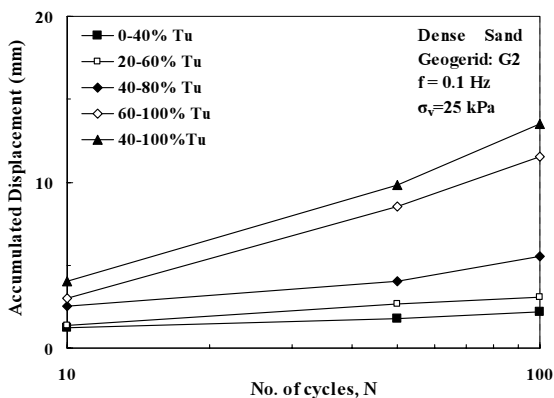


Fig. 9. Effect of number of cycles on frontal displacement

accumulation increases are linear and parallel in all cases. The linear relationship in log-scale indicates the decreasing increment of displacements with cycles. The parallel lines are indication of an accumulation rule for the sand-geogrid in the particular sand density state. Legend of Fig. 9 shows the top and bottom limit of cycling loading; for example, 20-60%  $T_u$  indicates that cycles start at  $T_1=0.2T_u$  with amplitude of  $60-20=40\%$  of  $T_u$ .

As stated in sample preparation section, telltale type instruments were installed along the specimen at the position of four transverse ribs. Figure 10 presents the displacement and strain distribution along the embedded length of geogrid G2 in dense sand under surcharges of 25, 50 and 100 kPa. It is observed that the trend of the results in cyclic and monotonic tests is similar to each other. In legend of Fig. 10,  $u_1$  is the frontal displacement and six curves in these graphs indicate six levels or state during pullout test; For example  $u_1=30$  mm shows displacement and strain distribution at time that frontal displacement of geogrid has reached to 30 mm. According to presented graphs in Fig. 10, with increase in vertical surcharge, the displacement at nodes decreased, but increase in tensile force along the geogrid cause increase in stain.

The relationship between the clamp displacement,  $\Delta_c$ , and the end rib displacement,  $\Delta_e$ , for geogrid G2 in dense sand and different surcharges are illustrated in Fig. 11 and is observed that end rib displacement is decreased with increasing of normal pressure. It is clear that the equality of frontal and end rib displacement, i.e.

$\Delta_c=\Delta_e$ , conduce the sliding of geogrid and difference between those, representatives the tensile displacement of reinforcement. According to Fig. 11, it is observed that under high values of normal surcharges, difference between  $\Delta_c$  and  $\Delta_e$  is increased and sliding of reinforcement has replaced by tension displacement and consequently increasing of strain or tensile force in it.

## 5. Conclusions

Monotonic and cyclic pullout tests were performed on two high-strength HDPE geogrids G1 and G2, with strength ratio of 1 to 2, embedded in dense and loose state conditions of silica sand with fairly uniform particle size distribution under different vertical surcharges. The main objective of the study was the behavior of pullout resistance of the geogrid with special focus on strength and deformation responses. The most important findings of the study are summarized below:

- Structural stiffness of geogrid has a direct effect on pullout resistance, in particular with increase in rate magnitude under lower vertical surcharges.
- The variation of post-cyclic resistance ranges from minus 10% under high surcharge, to plus 20% under low surcharge, of monotonic strength values.
- Repeatable unloading/reloading results in increase of pullout resistance, but accumulation of displacements results in instability. The unloading/reloading stiffness is constant at different load levels for practical applications.
- Displacement increments are high during the first few cycles but they rapidly reduce with increasing the number of cycles. The accumulated displacements are smaller for the high-strength geogrids.
- In loose sand condition, the cyclic accumulated displacements are considerably smaller as compared to dense sand condition. This might be related to the lower mobilized load levels in loose condition.
- The strain and tensile stress distribution trends along the geogrid specimen are similar in

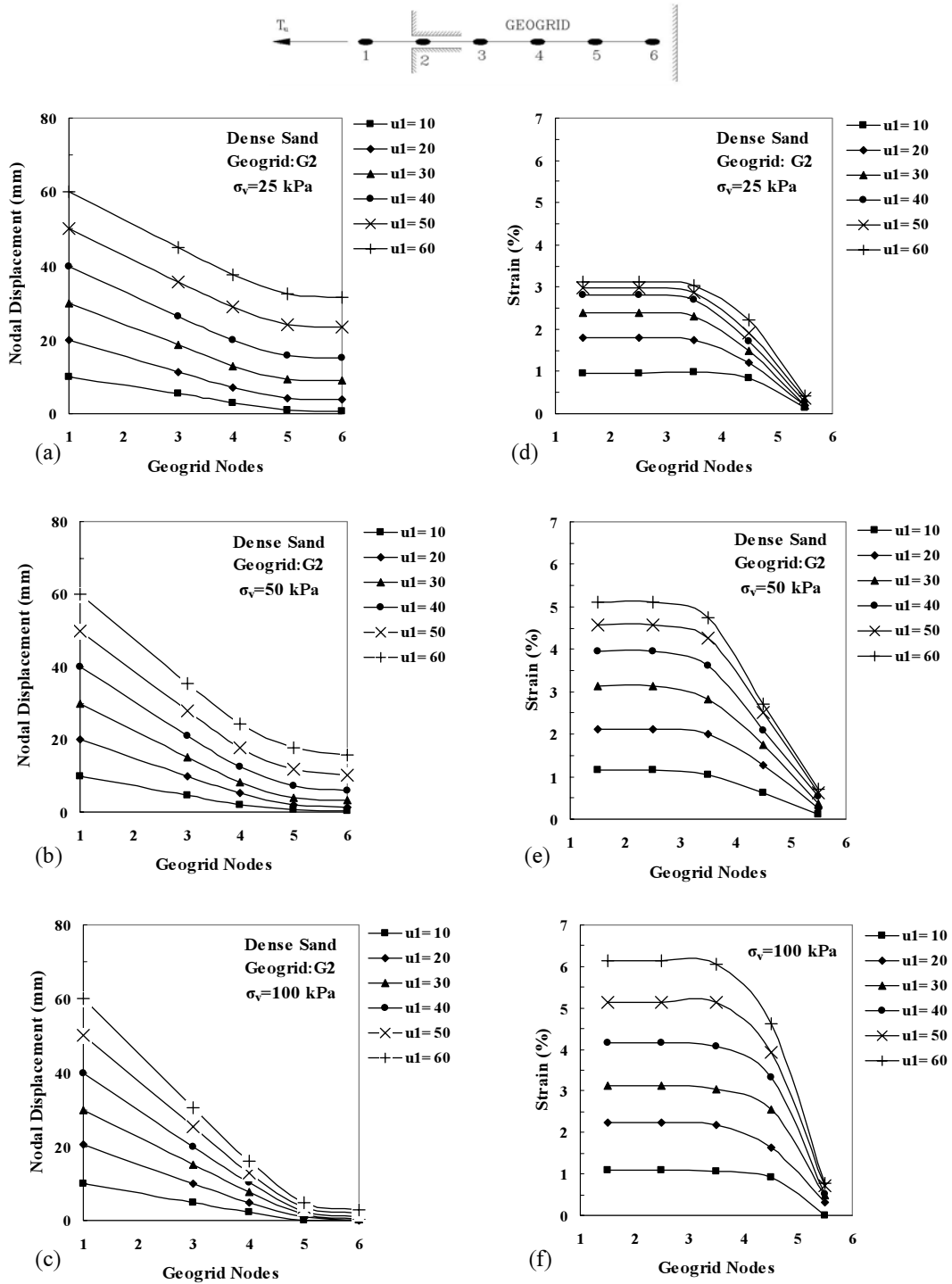


Fig. 10. Nodal displacement and strain distribution along embedded length of geogrid G2 in dense sand

monotonic and cyclic loading and decrease non-linearly along the embedded length of geogrid; further sliding of geogrid has replaced by tension of it under high level of vertical stress.

The observed post-cyclic pull-out resistance and cyclic accumulated displacement variation is not conducive to instability. Nevertheless, in practice real prototype conditions should be

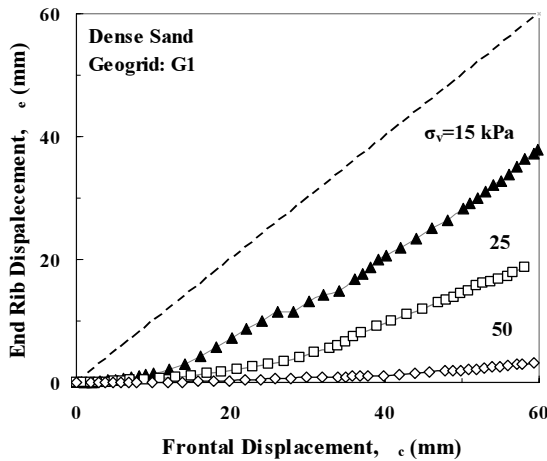


Fig. 11. Relationship between frontal and end rib displacement of geogrid G2

considered; since repetition of cyclic loads, in huge numbers under unexpected conditions of amplitude or load level, could reduce the overall stability of structures and further studies are underway considering these effects.

## References

- [1] Anderson, L.R., Nielsen, M.R., 1984. Pullout resistance of wire mats embedded in soil. Report for the Hilfiker Company from the Civil and Environmental Engineering Department of Utah State University, Logan Utah.
- [2] Jewell, R.A., Milligan, G.W.E., Sarsby, R.W., Dubois, 1984. Interaction between soil and geogrids. Proceedings of Symposium on Polymer Grid Reinforcement in Civil Engineering. London, pp. 19-29.
- [3] Chai, J.C., 1992. Interaction between grid reinforcement and cohesive-frictional soil and performance of reinforced wall/embankment on soft ground. D. Engineering Dissertation. Asian Institute of Technology, Bangkok, Thailand.
- [4] Johnston, R.S., Romstad, K.M., 1989. Dilatation and boundary effects in large scale pull-out tests. Proceeding of 12th International Conference on soil Mechanics and Foundation Engineering, vol. 2, Rio De Janeiro, Brazil, pp. 1263-1266.
- [5] Farrag, K., Acar, Y.B., Juran, I., 1993. Pullout resistance of geogrid reinforcements. Geotextiles and Geomembranes 12, 133-159.
- [6] Sugimoto, M., Alagiyawanna, A.M.N., Kadoguchi, K., 2001. Influence of rigid and flexible face on geogrid pullout tests. Geotextiles and Geomembranes 19, 257-277.
- [7] Palmeira, E.M., Milligan, G.W.E., 1989. Scale and other factors affecting the results of pull-out tests of grid buried in sand. Géotechnique 11 (3), 511-524.
- [8] Lopes, M.L., Ladeira, M., 1996. Role of specimen geometry, soil height and sleeve length on the pull-out behaviour of geogrids. Geosynthetics International 3 (6), 701-719.
- [9] Lopes, M.J., Lopes M.L., 1999. Soil-geosynthetic interaction-Influence of soil particle size and geosynthetic structure. Geosynthetics International, 6(4), pp. 261-282.
- [10] Moraci, N., Recalcati, P., 2006. Factors affecting the pullout behavior of extruded geogrids embedded in a compacted granular soil. Geotextiles and Geomembranes 24, 220-242.
- [11] Teixeira, S.H.C., Bueno, B.S., Zornberg, J.G., 2007. Pullout resistance of individual longitudinal and transverse geogrid ribs. Journal of Geotechnical and Geoenvironmental Engineering, ASCE, 133 (1): 37-50.
- [12] Christopher, B.R., Gill, S.A., Giround, J.P., Juran, I., Mitchell, J.K., Schlosser, F., Dunncliff, J., 1990. Design and construction guidelines for reinforced soil structures. vol. 1. Federal Highways Administration, U.S. Department of Transportation, Report No. FHWA RD-89-043.
- [13] Yasuda, S., Nagase, H., Mauri, H., 1992. Cyclic pull-out tests of geogrids in soils. International proceeding of earth reinforcement practice, Kyushu, Japan. Edited by H. Ochiai, S. Hayashi, and J. Otani. A.A. Balkema, Rotterdam, the Netherlands, pp. 185-190.
- [14] Raju, D.M., Fannin, R.J., 1998. Load-strain-displacement response of geosynthetics in monotonic and cyclic pullout. Canadian Geotechnical Journal 35, 183-193.
- [15] Nernheim, A. Meyer, N., 2004. Cyclic pull-out tests on geogrids. International Conference on Geotechnical Engineering (ICGE) in sharjah, United Arab Emirates, S. 339-346.
- [16] ASTM D 6706-01, 2001. Standard test method for measuring geosynthetic pullout resistance in soil. ASTM, Philadelphia, PA, USA.